Real-Life Disease Monitoring in Follicular Lymphoma Patients Using Liquid Biopsy Ultra-Deep Sequencing and PET/CT

Ana Jiménez-Ubieto
Hospital 12 de Octubre
Maria Poza
Hospital Universitario 12 de Octubre
Alejandro Martin
Altum sequencing Co,
Yanira Ruiz-Heredia
Hospital Universitario 12 de Octubre
Sara Dorado
Altum Sequencing Co https://orcid.org/0000-0002-4144-0315
Gloria Figaredo
Hospital General Universitario de Toledo
Juan Manuel Rosa-Rosa
Instituto de Investigación Hospital 12 Octubre, i+12, Madrid, Spain
Antonia Rodriguez
Hospital 12 de Octubre
Carmen Barcena
Hospital Universitario 12 de Octubre
Laura Parrilla-Navamuel
Hospital General Universitario de Toledo
Jaime Carrillo
Altum Sequencing Co
Ricardo Sanchez Perez
Hospital U 12 Octubre https://orcid.org/0000-0002-6383-0381
Laura Rufian
Instituto de Investigación Hospital 12 Octubre, i+12, Madrid, Spain
Alexandra Juarez
Altum Sequencing Co
Margarita Rodriguez
Hospital Universitario 12 de Octubre
Chonwu Wang

Hosea Precision Medical Technology Co., Ltd., Weihai, Sh
Paula de Toledo
Computer Science and Engineering Department, Carlos III University, Madrid, Spain
Carlos Grande
Hospital Universitario 12 de Octubre
Manuela Mollejo
Hospital Virgen de la Salud
Luis Casado
Hospital Virgen de la Salud
Maria CALBACHO
Hospital Universitario 12 de Octubre
Tycho Baumann
Hospital Clinic
Inmaculada Rapado
University Hospital 12 Octubre and IIS (i+12)
Miguel Gallardo
H12O-CNIO Haematological Malignancies Clinical Research Unit, CNIO. https://orcid.org/0000-0002-3699-9130
Pilar Sarandeses
Hospital Universitario 12 de Octubre
Rosa Ayala
Hospital Universitario 12 de Octubre
Joaquín Martínez-López
Hospital Universitario 12 de Octubre
Santiago Barrio (Santibarrio0.3@gmail.com)
Hospital Universitario 12 de Octubre

Article

Keywords: Follicular Lymphoma, Liquid Biopsy, PET/CT, Minimal Residual Disease, cfDNA

Posted Date: August 3rd, 2022

DOI: https://doi.org/10.21203/rs.3.rs-1914377/v1

Version of Record: A version of this preprint was published at Leukemia on January 3rd, 2023. See the published version at https://doi.org/10.1038/s41375-022-01803-x.

Abstract

In the present study, we screened 84 Follicular Lymphoma patients for somatic mutations suitable as liquid biopsy MRD biomarkers using a targeted next-generation sequencing (NGS) panel. We found trackable mutations in 95% of the lymph node samples and 80% of the liquid biopsy baseline samples. Then, we use an ultra-deep sequencing approach with $2 \cdot 10^{-4}$ sensitivity (LiqBio-MRD) to track those mutations on 156 follow-up liquid biopsy samples from 55 treated patients. Positive LiqBio-MRD correlated with a higher risk of progression both at the interim evaluation (HR 13.0, 95% CI 2.70–63.4, $p < 0.001$) and at the end of treatment (EOT, HR 14.3, 95% CI 4.4–46.4, $p < 0.001$). Similar results were observed by PET/CT Deauville score, with a median PFS of 19 months vs. NR ($p < 0.001$) at the interim and 13 months vs. NR ($p < 0.001$) at EOT. LiqBio-MRD and PET/CT combined identified the patients that progressed in less than two years with 89% sensitivity and 100% specificity. Our results demonstrate that LiqBio-MRD is a robust and non-invasive approach, complementary to metabolic imaging, for identifying FL patients at high risk of failure during the treatment and should be considered in future response-adapted clinical trials.

Introduction

Follicular lymphoma (FL) is the second most common non-Hodgkin lymphoma in developed countries (1). It is genetically characterized by an upregulation of BCL2 in the progenitor B cell that transforms into a proliferating clone driven by t(14;18) translocations(2). Nowadays, FL is considered an indolent disorder with a relatively favorable course. Long remissions are often achieved with modern day treatments, with median survival rates approaching 20 years (3, 4). However, 15–20% of patients are primary refractory or progress during the first two years after first-line therapy (POD24). These patients present a poor outcome, with 5-year overall survival (OS) probabilities between 38% and 50% (5, 6).

The disease is characterized by a remitting, relapsing clinical course with progressive shortening of response duration after treatment. Moreover, high-grade transformation (HT) to more aggressive lymphoma occurs in around 3% of the patients per year (7–10). Global research efforts have been aimed at identifying patients with a high risk of progression and transformation to optimize the duration of treatment response and to ease suffering and morbidity. Many clinical, molecular, pathological, and imaging biomarkers have been described and used to stratify/group FL patients into several risk categories at diagnosis (11–19). However, most of these tools remain inaccessible in daily practice and have not been adequately tested to select the best therapy.

For this reason, as the understanding of prognosis is crucial, the ultimate goal in a disease such as FL should be to develop tools and approaches to guide therapy. Current studies of risk-adapted therapy based on minimal residual disease (MRD) evaluation remain to be investigational in FL (20). At the molecular level, several studies have shown that MRD assessment is predictive of outcome. Most of these studies have focused on evaluating the BCL2/IgH rearrangements, quantified by polymerase chain reaction (PCR) in bone marrow or peripheral blood. The levels of circulating-free DNA fragments (cfDNA)

have also demonstrated predictive value (21, 22). However, unlike in diffuse large B cell lymphoma (DLBCL), in FL, there are no studies evaluating MRD based on tumoral cfDNA detection (23, 24).

In contrast, PET/CT using the 5-point scale Deauville criteria (D5PS) is well established, regardless of the treatment used (25, 26), to predict the outcome and attain complete metabolic response. Nevertheless, the use of PET/CT alone is hampered by its limited sensitivity and specificity, and the interpretation of the results is highly dependent on the evaluating radiologist (27, 28). Moreover, there is little information on interim PET/CT (26) and its combination with MRD for prognostic assessment (20, 29), and there are no studies that have used liquid biopsy NGS methods. Therefore, in this study, we aim to analyze the response to therapy in FL patients using ultra-deep sequencing of cfDNA and the D5PS scale PET/CT to identify, early on, those patients who have a high risk of relapse in less than 24 months (POD24).

Materials/subjects And Methods

Patient Cohort and Study Design

This study was designed as a prospective observational study. The cohort included 84 newly diagnosed, recurrent or transformed FL patients recruited from the routine clinical practice at the Hospital 12 de Octubre (H12O) in Madrid, Spain, and the Hospital Universitario de Toledo, Spain. One patient (FL5), suffered from a transformation 10 months after the first-line therapy started. After transformation, the patient was included as a transformed case (FL5t). Informed written consent of all patients was obtained according to the Declaration of Helsinki. The study inclusion criteria were; histological confirmation and the availability of enough biological material in sequential samples. Treatment was started according to the *Groupe d'Etude des Lymphomes Folliculaires* criteria (30), and imaging examinations were performed as ordinary clinical practice. Responsible physicians decided on the treatment regimen according to institutional and international guidelines. In all patients, DNA from lymph node biopsies and cfDNA was obtained before the treatment was started. Somatic mutations of these samples were selected as disease biomarkers for liquid biopsy MRD (LiqBio-MRD) analysis at follow-up time-points. The following biological materials were analyzed: DNA from formalin-fixed paraffin-embedded (FFPE) lymph node biopsies (n = 75) and cfDNA (n = 44) before treatment start, and follow-up cfDNA samples during chemo-immunotherapy courses (n = 156).

DNA extraction

Lymph node DNA was extracted with a Qiamp gDNA FFPE kit (Qiagen, Hilden, Germany) using two to four sections from 5 to 10 microns, cut from the original paraffin block. Then, the gDNA was eluted in 35 µL ATE buffer and quantified using the Qubit BR kit (Thermo Fisher Scientific, Waltham, Massachusett, USA). For cfDNA extraction, 10 to 20 mL peripheral blood was collected in EDTA tubes and processed in less than four hours at the H12O. Samples from Toledo were collected in Roche Cell-Free DNA collection Tubes (Roche Diagnostic, Basel. Switzerland) and sent to the H12O, where plasma separation and cfDNA purification were centralized. There were no differences in cfDNA quantity or quality observed between EDTA and Streck collection tubes. The plasma was separated with two centrifugation steps at 1600 g

and 4500g, and stored at -80°C until further use. The purification of cfDNA was performed with a Qiamp Circulating Nucleic Acid kit (Qiagen) and quantified using a Qubit HS kit (Thermo Fisher Scientific). Fragment size and genomic DNA contamination were quantified using a Bioanalyzer 2100 fragment analysis system (Agilent, Santa Clara, California. USA).

Baseline Genotyping and LiqBio-MRD Biomarker Selection

The lymph node gDNA and plasma cfDNA baseline samples were screened for mutations with a short-length Ampliseq Custom Panel (Thermo-Fisher). The panel, established as a routinary diagnosis tool at the H12O, was designed to cover all coding regions of 56 lymphoma-specific genes in the FFPE samples (Supplemental Table S1). Samples were sequenced with an average coverage of 2,150x on an Ion S5 System platform (Life Technologies, Thermo Fisher Scientific). Variant annotation was performed using the default annotate variants single sample workflow from the Ion Reporter software (version 5.18.2.0). Mutations were called when presented more than nine mutated reads and a Variant Allele Frequency (VAF) above $2 \cdot 10^{-2}$ (2%). In the case of FFPE samples, deamination-related base changes were reduced by filtering out C > T / G > A changes with a below $2 \cdot 10^{-1}$ (20%) and a transformed *p*-value greater than − 2, unless previously described as a somatic aberration in FL (COSMIC database). Only somatic mutations previously described in cancer, or variants of unknown significance (VUS) with relevant functional impact were used as MRD biomarkers (Supplemental Table S2).

LiqBio-MRD Methodology and Bioinformatic Pipeline

On average, 86.3 ng of cfDNA (rank 15–354 ng) was obtained from the initial 10–20 mL of peripheral blood (PB). All samples with a gDNA/cfDNA ratio greater than one were excluded. The minimum quantity of cfDNA sequenced was 15ng. Considering that a genome equivalent (GE) has a mass of 3pg (31), 15ng is enough to screen 5,000GE and therefore achieve a sensitivity of $2 \cdot 10^{-4}$ VAF (0.02%). In addition, five samples with less than 15ng of cfDNA but high disease burden and positive MRD value were included in the study.

To reduce the false positive rate, a strict bioinformatic pipeline was programmed in Python and R to eliminate low-quality reads. Moreover, a triplicate approach using molecular tagged primers and the definition of the limit of detection (LOD) in healthy control donors was performed on each MRD biomarker. First, a multiplexed mini-panel was defined for every patient with the specific MRD biomarkers identified at diagnosis. The mini-panel included the molecular-tagged primer pairs (6-mer tags) to amplify every mutation in three biological replicates defined as P1, P2, and P3. (Supplemental Table S3). After an initial amplification step with the tagged primers, the triplicates were combined in a single library and sequenced on the Ion Proton System platform (Life Technologies, Thermo Fisher Scientific Inc.) with an estimated depth of 500,000x per amplicon, as previously described (32). The FASTQ files produced after sequencing were automatically demultiplexed to separate the reads from the different amplicons and triplicates. Then, specific wild-type and mutated sequences were generated for each genetic position. These sequences, obtained from the corresponding demultiplexed output file, cover the affected locus with 15 bp upstream and downstream. Only the reads that perfectly match these sequences were

considered to calculate the VAF for each triplicate. The noise effects arising from PCR and sequencing were controlled by identifying and removing triplicates that overpassed the mean VAF plus one standard deviation (SD). Finally, the corrected VAF was compared with the LOD calculated for each mutation independently using three triplicates of three healthy donors. The LOD was computed as the VAF in control samples plus three times the SD. Every hotspot with a corrected mean VAF below the LOD was automatically eliminated. (Supplemental Table S3) The final LiqBio-MRD value was defined by the mutation with the highest VAF at the sampling time-point, as shown in Supplemental Figure S1.

PET/CT Imaging

The PET/CT scans were performed with a General Electric Discovery MI (GEDMI) Scanner or a Siemens Biograph 6 Scanner. PET/CT and CT images were acquired in the same session after injection of 2.5-3 MBq/kg ^{18}F-FDG (fluorodeoxyglucose) for the GEDMI Scanner and 4–5 MBq/kg ^{18}F-FDG for the Siemens scanner. All follow-ups were performed in the GEDMI scanner. CT scans obtained with a low-dose protocol were used for attenuation correction of the PET/CT images. Interim and EOT^{18}FDG-PET/CT scans were visually assessed according to the D5PS, with ^{18}FDG uptake of any residual lesion, using mediastinal blood pool and liver uptake as reference settings. PET/CT was considered to be positive when the Deauville's score was four or five, and Deauville's scores from one to three were classified as PET/CT negative.

In first-line therapy, PET/CT was performed before starting the treatment, after four cycles (n = 36), and at the end of treatment (EOT, n = 50). After finishing induction, patients were closely monitored with a physical examination and routine laboratory tests. A new scan was performed only when new symptoms or laboratory changes were detected. PET/CT was generally performed at mid-induction (n = 8) and EOT (n = 13) for patients treated in other lines. The exact time-points are listed in Supplemental Table S4.

Statistical Analysis

The Kruskal–Wallis test was used to determine statistically significant differences in the obtained samples' MRD values among the PET/CT-related categories. Then, a post hoc Dunn test was conducted to identify the statistically significant pairwise comparisons and the corresponding p-values. The tests were both performed using Python, the prior with the Python package SciPy (version 1.6.2) and the latter with the Python package scikit-posthocs (version 0.6.7). The Pearson correlation coefficient was used to assess the linear relationship between the different variables under study. Univariable Cox proportional hazards regression models and Kaplan–Meier survival analysis were performed to test statistical associations between genetic and imaging findings and survival outcomes. Statistical calculations were conducted using SPSS 22.0 (IBM SPSS Inc, Chicago). P-values of ≤ 0.05 were considered to be significant.

Results

Patients' Characteristics and Predictive Features

A total of 84 FL patients were included in the study. The median age was 63 years (35–90 years), and 58% of the patients were female. Eleven cases did not require treatment, 85% of the patients presented low histological grade (1–2), and 79% had advanced (III–IV) Ann Arbor stage (Table 1). Regarding treated cases ($n = 73$), 58 patients received first-line treatment (39 R-CHOP, 10 R-bendamustine, 4 rituximab monotherapy, and 5 radiotherapy). The other 15 patients were treated with salvage therapy (Supplemental Table S4). More important prognostic indexes in FL were analyzed. High-risk patients defined by FLIPI, FLIPI2, m7-FLIPI, and PRIMA PI did not show shorter PFS. Bulky disease, the presence of symptoms B, and a lymphocyte-to-monocyte ratio (LMR) of < 2.5 were the only variables associated with a higher risk of relapse ($p < 0.05$). After a median follow-up of 26 months, 18 pretreated patients relapsed after a median of 19 months (15 patients with grade I, II, or 3A and 3 patients transformed). Eight cases died after a median of 29 months (five patients had a low histological grade, and three patients were transformed). The causes for death were lymphoma in four cases (three transformed), infection ($n = 2$), and secondary neoplasia ($n = 1$).

Baseline Genotyping on cfDNA Complements Lymph Node Screening in Follicular Lymphoma

Baseline genotyping with the targeted NGS panel was performed in 75 lymph node samples and 44 cfDNA plasma samples. In the lymph node samples, 510 mutations were detected with an average of 6.8 somatic mutations per patient (range 0–31) and a mean VAF of 0.31 (range 0.026–1.0). In the cfDNA plasma samples, 144 mutations were detected (average 3.3, range 0–11) with a mean VAF of 0.22 (range 0.025–0.857). Only 4 of 75 (5%) lymph node samples did not present any alteration suitable for MRD monitoring. This number increased to 20% (9 of 44) when only baseline cfDNA was considered. However, for six of the eight patients without lymph node samples available, somatic mutations were detected in the cfDNA fraction.

As previously described (12), the most frequently mutated genes were *KMT2D*, *CREBBP*, *BCL2*, *TNFRSF14*, and *EZH2* (Fig. 1A). Although the samples from transformed patients had a similar genetic profile, an increase of *TP53* mutations was observed in this subcohort (3/10, 33% vs. 7/73, 9%, Supplemental Figure S2). Within the 36 cases with available paired lymph node and plasma samples, 88 somatic mutations were identified in both fractions, 33 somatic mutations were only detectable in liquid biopsy, and 160 somatic mutations were only in the lymph node (Supplemental Table S2, Supplemental Figure S4).

Clinical Impact of Disease Monitoring by LiqBio-MRD

The dynamics of the baseline mutations were analyzed on 156 cfDNA follow-up samples from 55 patients that received treatment (Fig. 1B). Additionally, sequential samples of eleven untreated "watch and wait" patients were screened. On average, 3.2 somatic mutations per patient (range 1–10) were

selected as MRD biomarkers. Seven mutations were excluded from further analyses as they presented a LOD above $1{\cdot}10^{-4}$. These mutations mainly affected insertions or deletions of one base (Supplemental Figure S4). On the other hand the elimination of outlier triplicates permited to identify and correct nine false positives follow-up samples. The LiqBio-MRD value was significantly lower in cases with complete response (CR) by PET/CT as compared with those within progression ($p < 0.001$). However, 14 out of 60 PET/CT negative samples were LiqBio-MRD positive. A similar result was obtained for the time-points (TP) in partial response and stable disease (Fig. 1C). All samples collected before treatment and those from untreated patients (18 samples from 13 patients) were positive by the LiqBio-MRD test.

The 55 screened patients presented an average of three sequential liquid biopsy samples available (rank (1–8). To calculate the clinical impact of the LiqBio-MRD test, we defined three different timeframe groups: Early follow-up ($n = 25$) included cfDNA samples from cycles I and II; the interim group ($n = 28$) included samples obtained in cycles III and IV; the final or EOT group included 42 cfDNA samples obtained in cycle VI or the first sample available under maintenance (Fig. 2, left). Positive LiqBio-MRD values in the early group did not increase the risk of progression (HR_{EARLY} 2.9, 95%, CI 0.59–14.6, $p = 0.157$). This tendency changed at interim monitoring (HR_{INT} 13.0, 95% CI 2.70–63.4, $p < 0.001$). The differences between LiqBio-MRD positive and negative cases were even more pronounced at EOT (HR_{EOT}, HR 14.3, 95% CI 4.4–46.4, $p < 0.001$), Fig. 2, right).

Interim Monitoring by LiqBio-MRD and PET/CT of Previously Untreated Patients Predicts Progression

When only previously untreated patients were considered, LiqBio-MRD and PET/CT D5PS tests showed prognostic value. At the interim evaluation, LiqBio-MRD positive patients presented a median PFS_{INT} of 14 months vs. NR (not reached) for negative cases ($p < 0.001$, Fig. 3A). PET/CT positive cases had a $mPFS_{INT}$ of 19 months vs. NR ($p < 0.001$, Fig. 3B). Comparable results were observed at EOT ($mPFS_{EOT}$ LiqBio-MRD 13 months vs. NR, $p < 0.001$; $mPFS_{EOT}$ PET/CT 13 months vs. NR, $p < 0.001$, Fig. 3C,D), and when transformed cases were excluded (Supplemental Figure S5). Of note, the distribution of cases according to interim and EOT TPs for PET/CT and LiqBio-MRD presented a concordance of 76% (Kappa = 0.401).

The Combination of LiqBio-MRD and PET/CT Identifies POD24 Patients

Next, we studied the 50 patients with data on both PET/CT and LiqBio-MRD. The last TP (interim or EOT) with available data for both tests was considered for this analysis. Twenty-eight patients were negative by both techniques, eight patients were positive, and 14 patients presented discordant results. Considering only concordant results ($n = 36$), the combination of both tests showed a sensitivity (SE) of 89% and a specificity (SP) of 100%, with a PPV of 100% and NPV of 96.4%. Strikingly, all positive patients by both tests had a 2-year PFS below 24 months (mPFS of 7 months for +/+ vs. NA for -/- cases, $p <$

0.001, Fig. 4). Moreover, the only case (FL25) that progressed with a negative result by both tests, was positive in a sequential cfDNA sample obtained at maintenance, five months before progression. Regarding the 14 cases with discordant results (25%), 10 patients were incorrectly classified by PET/CT, and only 4 patients were incorrectly classified by LiqBio-MRD (Fig. 4). The results generated at EOT, and only including not transformed first-line patients, are shown in Supplemental Figure S6.

Other approaches for disease monitoring were also tested. Flow cytometry data was only available for 11 patients with bone marrow infiltration. Two patients were positive at follow-up and nine patients were negative at follow-up, concurring at 100% with PET/CT and LiqBio-MRD. The BCL2/IgH rearrangements were screened in 33 patients with peripheral blood samples available. Rearrangements were only detected at baseline diagnosis for ten of the patients, being all negative in follow-up samples. Two of these cases were positive by PET/CT and LiqBioMRD, four cases presented discordant results, and three cases were negative by both tests.

Dynamics of Somatic Mutations during the Follow-up of FL Patients

As indicated above, only one patient (FL25) had a negative result by PET/CT and LiqBio-MRD at interim and EOT and eventually progressed. Three somatic mutations affecting *KMT2D*, *CREBBP*, and *ARID1A* were found in this case. Of interest, this patient was MRD negative in three TPs obtained during the first year but had a positive LiqBio-MRD sample obtained 15 months after the start of treatment. An additional positive liquid biopsy was received three months later, and PET/CT was performed, confirming progression but with a low tumor burden (Fig. 5A). The patient continued maintenance therapy, achieving a complete response a few months later.

The opposite dynamics were observed in patient FL5. This patient did not respond to RCHOP (DS5) and received R-bendamustine as second-line therapy. The interim PET/CT showed a poor response (DS5), and the biopsy confirmed the transformation to high-grade lymphoma. After failure of rescue treatment with R-GEMOX-dexamethasone and R-polatuzumab bendamustine, the patient received radiotherapy where a reduction in the main clone was observed (Fig. 5B). Of note, the clone detected in cfDNA disappeared under first-line therapy.

Patient FL30 presented two mutations detected only in lymph node and two more only detected in cfDNA. In follow-up samples, the four mutations were undetectable. In the PET/CT evaluation, a residue was observed in the scans, complicating the interpretation of the imaging results (Fig. 5C). This patient is still in CR after two years of follow-up.

Although a solid biopsy was unavailable for patient FL31, six somatic mutations were detected in the baseline liquid biopsy sample. In follow-up cfDNA samples, despite an initial reduction during the first two cycles, a rapid increase in the disease burden after cycle III was observed. The patient progressed in cycle VI and died under rescue therapy only nine months from the start of the treatment (Fig. 5D). The

dynamics of all the treated patients with follow-up samples available are shown in Supplemental Figure S7.

Discussion

This prospective study evaluates, for the first time, the usefulness of liquid biopsy MRD by ultra-deep sequencing in combination with D5PS PET/CT to identify, early on, those FL patients with a high risk of relapse in less than 24 months (POD24). Our approach is based on the use of somatic mutations as disease biomarkers, as we previously described for acute myeloid leukemia (32). First, we screened baseline lymph node and plasma samples to identify patient specific biomarkers. The genetic profile of our cohort mimics the one previously described by Pastore et al. (12) but with an expected increase of *TP53* alterations in transformed cases (33) (Supplemental Figure S1). Although the custom DNA panel was initially designed for FFPE samples, the small amplicon size permitted the detection of lymphoma-specific mutations in baseline liquid biopsies (Fig. 1A). In our study, limited by the follow-up and the small and heterogeneous number of subjects, the only clinically relevant prognostic factor for PFS in newly diagnosed patients ($n = 84$) was the low lymphocyte-to-monocyte ratio (19). We did not find prognostic differences by applying IPI, FLIPI, FLIPI2, m7-FLIPI, or PRIMA IPI. However, somatic mutations suitable for LiqBio-MRD monitoring were found in 95% of patients with lymph node samples and 80% of patients with plasma samples. These values considerably improve the applicability of MRD assessment as compared with other described techniques, such as PCR of the IGH/BCL2 translocation (20, 29). Although PCR-positive is predictive of lower PFS, a considerable number of patients are t(14;18) negative (60%). Moreover, FL is a predominantly nodal disease, and the absence of t(14;18) in bone marrow does not adequately reflect the response status (41). Further, t(14;18) can also be found in healthy individuals at low level.

In this study, LiqBio-MRD was evaluated in the plasma of 55 patients that received treatment (43 first-line therapy). The analysis, performed in 156 follow-up cfDNA samples allowed us to define patient-specific disease dynamics (Fig. 1B, Supplemental Figure S7) and their correlation with the clinical outcome (Fig. 1C). To the best of our knowledge, there are no studies in FL evaluating early MRD assessed by liquid biopsy. Conversely, there are already some studies in DLBCL (24, 34, 35) and Hodgkin lymphoma (36) where it is known that levels often change rapidly after the initiation of therapy. Following this hypothesis in FL, we performed an early LiqBio-MRD evaluation (Cycle 2) on 26 patients. Although a trend to shorter PFS was observed in MRD positive cases, 6 of 13 cases eventually became negative at later time-points (Fig. 2), suggesting that FL presents a different dynamic than DLBCL (38) and treatment need longer to cleanse the tumor.

Since the Lugano classification, the criteria to determine the quality of treatment response rely on the D5PS PET/CT evaluation (37). Several studies, including large retrospective subanalyses of randomized trials have shown that PET/CT negativity correlates solidly with PFS (25, 38). Nevertheless, the use of PET/CT alone is hampered by its limited sensitivity and specificity and the interpretation of the results being highly dependent on the evaluating radiologist (27, 39). Consistent with previous reports (23), from

the 64 patients with available PET/CT scans (50 patients in first-line therapy), 70% of the patients reached a CR.

On the other hand, the LiqBio-MRD test showed an extraordinary capacity to identify patients at risk of progression after only four cycles of RCHOP (Fig. 3A), even if relapsed or transformed FL patients were removed from the analysis (Supplemental Figure S5). Comparable results were observed by interim PET/CT (Fig. 3B). This result suggests that LiqBio-MRD or PET/CT interim evaluation should be considered in future clinical trial settings. Regarding EOT evaluation, both tests segregated high-risk patients (Fig. 3C, D). Although similar results have already been shown in FL patients using PCR-based MRD techniques, these approaches were hampered by a lower applicability (20, 29, 40–42).

PET/CT has only been used in combination with PCR in a small exploratory analysis and MRD refined the predictive power of PET/CT (29). However, no combination of PET/CT and MRD strategies has been reported using NGS liquid biopsy techniques. In our study, the combination of both methods identified 100% of the POD24 patients. As shown in Fig. 4, patients with concordant results ($n = 36$) were almost perfectly segregated. These results remained when only the first line EOT evaluation was considered after excluding transformed cases (Supplemental Figure S6). The only double negative patient (FL25, Fig. 5A) that progressed presented an increase in tumor burden detectable by LiqBio-MRD five months before progression in a sample obtained within maintenance. This suggests that sequential monitoring with a minimally invasive test such as LiqBio-MRD may be essential to identify POD24 cases and anticipate patients' relapses. Another interesting case, FL5, illustrates how LiqBio-MRD may have other possible applications (Fig. 5B). In this chemo-refractory patient, radiotherapy had an abscopal effect, confirmed by the rapid descend of ctDNA not otherwise explicated (43).

Our study has several of limitations, including the limited number of patients, the heterogenous treatment administered, and the absence of available tests in all the time-points. However, several factors permitted the development of a LiqBio-MRD test with extraordinary performance. First, the MRD amplicons were designed shorter than 120bp and all MRD samples screened presented at least 15ng of cfDNA to guaranty the amplification of enough tumor cfDNA molecules. More importantly, the use of triplicates and the definition of LOD in healthy control donors permitted to identify and correct the false positive values induced by PCR and sequencing errors or the variant intrinsic noise due to the genetic context. Although it seems mandatory to perform larger studies to confirm this preliminary data, our results demonstrate, for the first time, that NGS-based MRD quantification is feasible in liquid biopsies from FL. The achievement of negative ctDNA after treatment and in an interim analysis enhances prognostic information on the patients´ outcomes, both in first-line therapy and at relapse. PET/CT and LiqBio-MRD can synergistically contribute to predicting progression and POD24 with high sensitivity and specificity. Additionally, this test better reflects intra-patient tumor heterogeneity (44, 45) and could be used to detect drug resistance and high-risk transformation and guide and monitor treatment.

In conclusion, LiqBio-MRD monitoring in FL represents a promising option, complementary to metabolic imaging, to identify patients at high risk of failure early on during treatment and is a useful approach to

response-adapted precision therapy to be considered in clinical trials.

Declarations

Acknowledgements

This study has been funded by Instituto de Salud Carlos III (ISCIII) and co-funded by the European Union through the projects PI21/00314, PI 19/01430, PI19/01518 and PI18/00295, PTQ2020-011372, CP19/00140, CP22/00082, Doctorado industrial CAM IND2020/TIC-17402 and CRIS cancer foundation.

Author Contributions

AJU, MP, IR, MG, RA, JML and SB designed the research. JC, RS, LR, AJ and MR performed the experiments. AM, YR, SD and JMR, CW, PT and SB defined the bioinformatic pipeline and performed sequencing data analysis. AJU, MP, GF, AR, CB, LPN, CG, MM, LFC, MC, TB, MG, PS and RS provided patient samples and clinical data. All authors analyzed and interpreted the data. AJU, MP, AM and SB wrote the manuscript which was approved by all authors.

Competing Interests

RA, JML and SB are equity shareholders of Altum Sequencing Co. LFC received honoraria and received research funding from Roche, Novartis, Astra Zeneca, Janssen, BMS, Pfizer and Incyte. The remaining authors declare no competing financial interests.

Data Availability Statement

The datasets generated during and/or analysed during the current study are available from the corresponding author on reasonable request.

References

1. Anderson JR, Armitage JO, Weisenburger DD. Epidemiology of the non-Hodgkin's lymphomas: Distributions of the major subtypes differ by geographic locations. Ann Oncol. 1998 Jul;9(7).
2. Küppers R, Stevenson FK. Critical influences on the pathogenesis of follicular lymphoma. Blood. 2018 May 24;131(21):2297–306.
3. Cheah CY, Chihara D, Ahmed M, Davis RE, Nastoupil LJ, Phansalkar K, et al. Factors influencing outcome in advanced stage, low-grade follicular lymphoma treated at MD Anderson Cancer Center in the rituximab era. Ann Oncol. 2016 May;27(5).
4. Jiménez-Ubieto A, Grande C, Caballero D, Yáñez L, Novelli S, Hernández-Garcia MT, et al. Autologous Stem Cell Transplantation for Follicular Lymphoma: Favorable Long-Term Survival Irrespective of Pretransplantation Rituximab Exposure. Biol Blood Marrow Transplant. 2017 Oct;23(10).

5. Jiménez-Ubieto A, Grande C, Caballero D, Yáñez L, Novelli S, Hernández MT, et al. Progression-free survival at 2 years post-autologous transplant: a surrogate end point for overall survival in follicular lymphoma. Cancer Med. 2017 Dec 1;6(12):2766–74.
6. Casulo C, Dixon JG, Le-Rademacher J, Hoster E, Hochster H, Hiddemann W, et al. Validation of POD24 As a Robust Early Clinical Endpoint of Poor Survival in FL from 5,225 Patients on 13 Clinical Trials. Blood. 2021 Oct 6;
7. Pasqualucci L, Khiabanian H, Fangazio M, Vasishtha M, Messina M, Holmes AB, et al. Genetics of Follicular Lymphoma Transformation. Cell Rep. 2014;6(1):130–40.
8. Sarkozy C, Trneny M, Xerri L, Wickham N, Feugier P, Leppa S, et al. Risk factors and outcomes for patients with follicular lymphoma who had histologic transformation after response to first-line immunochemotherapy in the PRIMA trial. J Clin Oncol. 2016 Aug 1;34(22):2575–82.
9. Sorigue M, Mercadal S, Alonso S, Fernández-Álvarez R, García O, Moreno M, et al. Refractoriness to immunochemotherapy in follicular lymphoma: Predictive factors and outcome. Hematol Oncol. 2017 Dec 1;35(4):520–7.
10. Alonso-Álvarez S, Magnano L, Alcoceba M, Andrade-Campos M, Espinosa-Lara N, Rodríguez G, et al. Risk of, and survival following, histological transformation in follicular lymphoma in the rituximab era. A retrospective multicentre study by the Spanish GELTAMO group. Br J Haematol. 2017 Sep 1;178(5):699–708.
11. Okosun J, Bödör C, Wang J, Araf S, Yang CY, Pan C, et al. Integrated genomic analysis identifies recurrent mutations and evolution patterns driving the initiation and progression of follicular lymphoma. Nat Genet. 2014 Feb;46(2):176–81.
12. Pastore A, Jurinovic V, Kridel R, Hoster E, Staiger AM, Szczepanowski M, et al. Integration of gene mutations in risk prognostication for patients receiving first-line immunochemotherapy for follicular lymphoma: A retrospective analysis of a prospective clinical trial and validation in a population-based registry. Lancet Oncol. 2015 Sep 1;16(9):1111–22.
13. Jurinovic V, Kridel R, Staiger AM, Szczepanowski M, Horn H, Dreyling MH, et al. Clinicogenetic risk models predict early progression of follicular lymphoma after first-line immunochemotherapy. Blood. 2016 Aug 25;128(8):1112–20.
14. Meignan M, Cottereau AS, Versari A, Chartier L, Dupuis J, Boussetta S, et al. Baseline metabolic tumor volume predicts outcome in high-tumor-burden follicular lymphoma: A pooled analysis of three multicenter studies. In: Journal of Clinical Oncology. American Society of Clinical Oncology; 2016. p. 3618–26.
15. Cottereau AS, Versari A, Chartier L, Dupuis J, Tarantino V, Casasnovas R-O, et al. Low Suvmax Measured on Baseline FDG-PET/CT and Elevated β2 Microglobulin Are Negative Predictors of Outcome in High Tumor Burden Follicular Lymphoma Treated By Immunochemotherapy: A Pooled Analysis of Three Prospective Studies. Blood. 2016 Dec 2;128(22):1101–1101.
16. Bachy E, Maurer MJ, Habermann TM, Gelas-Dore B, Maucort-Boulch D, Estell JA, et al. A simplified scoring system in de novo follicular lymphoma treated initially with immunochemotherapy. Blood.

2018 Jul 5;132(1):49–58.

17. Huet S, Tesson B, Jais JP, Feldman AL, Magnano L, Thomas E, et al. A gene-expression profiling score for prediction of outcome in patients with follicular lymphoma: a retrospective training and validation analysis in three international cohorts. Lancet Oncol. 2018 Apr 1;19(4):549–61.
18. Mir F, Barrington SF, Brown H, Nielsen T, Sahin D, Meignan M, et al. Baseline SUVmax did not predict histological transformation in follicular lymphoma in the phase 3 GALLIUM study. Blood. 2020 Apr 9;135(15):1214–8.
19. Mozas P, Rivero A, Rivas-Delgado A, Nadeu F, Clot G, Correa JG, et al. A low lymphocyte-to-monocyte ratio is an independent predictor of poorer survival and higher risk of histological transformation in follicular lymphoma. Leuk Lymphoma. 2021;62(1):104–11.
20. Luminari S, Manni M, Galimberti S, Versari A, Tucci A, Boccomini C, et al. Response-Adapted Postinduction Strategy in Patients With Advanced-Stage Follicular Lymphoma: The FOLL12 Study. J Clin Oncol. 2022 Mar 1;40(7):729–39.
21. Delfau-Larue MH, Van Der Gucht A, Dupuis J, Jais JP, Nel I, Beldi-Ferchiou A, et al. Total metabolic tumor volume, circulating tumor cells, cell-free DNA: Distinct prognostic value in follicular lymphoma. Blood Adv. 2018 Apr 10;2(7):807–16.
22. Sarkozy C, Huet S, Carlton VEH, Fabiani B, Delmer A, Jardin F, et al. The prognostic value of clonal heterogeneity and quantitative assessment of plasma circulating clonal IG-VDJ sequences at diagnosis in patients with follicular lymphoma. Oncotarget. 2017 Jan 31;8(5):8765–74.
23. Kurtz DM, Green MR, Bratman S V., Scherer F, Liu CL, Kunder CA, et al. Noninvasive monitoring of diffuse large B-cell lymphoma by immunoglobulin high-throughput sequencing. Blood. 2015 Jun 11;125(24):3679–87.
24. Kurtz DM, Soo J, Co Ting Keh L, Alig S, Chabon JJ, Sworder BJ, et al. Enhanced detection of minimal residual disease by targeted sequencing of phased variants in circulating tumor DNA. Nat Biotechnol 2021 3912. 2021 Jul 22;39(12):1537–47.
25. Trotman J, Barrington SF, Belada D, Meignan M, MacEwan R, Owen C, et al. Prognostic value of end-of-induction PET response after first-line immunochemotherapy for follicular lymphoma (GALLIUM): secondary analysis of a randomised, phase 3 trial. Lancet Oncol. 2018 Nov 1;19(11):1530–42.
26. Dupuis J, Berriolo-Riedinger A, Julian A, Brice P, Tychyj-Pinel C, Tilly H, et al. Impact of [18F]fluorodeoxyglucose positron emission tomography response evaluation in patients with high-tumor burden follicular lymphoma treated with immunochemotherapy: A prospective study from the Groupe d'Etudes des Lymphomes de l'Adulte and GOELAMS. J Clin Oncol. 2012 Dec 10;30(35):4317–22.
27. Han HS, Escalón MP, Hsiao B, Serafini A, Lossos IS. High incidence of false-positive PET scans in patients with aggressive non-Hodgkin's lymphoma treated with rituximab-containing regimens. Ann Oncol. 2009 Feb 1;20(2):309–18.
28. Ansell SM, Armitage JO. Positron emission tomographic scans in lymphoma: Convention and controversy. In: Mayo Clinic Proceedings. Elsevier Ltd; 2012. p. 571–80.

29. Luminari S, Galimberti S, Versari A, Biasoli I, Anastasia A, Rusconi C, et al. Positron emission tomography response and minimal residual disease impact on progression-free survival in patients with follicular lymphoma. A subset analysis from the FOLL05 trial of the fondazione italiana linfomi. Vol. 101, Haematologica. Ferrata Storti Foundation; 2016. p. e66–8.
30. Brice P, Bastion Y, Lepage E, Brousse N, Haïoun C, Moreau P, et al. Comparison in low-tumor-burden follicular lymphomas between an initial no-treatment policy, prednimustine, or interferon alfa: a randomized study from the Groupe d'Etude des Lymphomes Folliculaires. Groupe d'Etude des Lymphomes de l'Adulte. J Clin Oncol. 1997;15(3):1110–7.
31. Dang DK, Park BH. Circulating tumor DNA: current challenges for clinical utility. J Clin Invest. 2022 Jun 15;132(12).
32. Onecha E, Linares M, Rapado I, Ruiz-Heredia Y, Martinez-Sanchez P, Cedena T, et al. A novel deep targeted sequencing method for minimal residual disease monitoring in acute myeloid leukemia. Haematologica. 2019 Jan 31;104(2):288.
33. Bouska A, McKeithan TW, Deffenbacher KE, Lachel C, Wright GW, Iqbal J, et al. Genome-wide copy-number analyses reveal genomic abnormalities involved in transformation of follicular lymphoma. Blood. 2014 Mar 13;123(11):1681–90.
34. Kurtz DM, Scherer F, Jin MC, Soo J, Craig AFM, Esfahani MS, et al. Circulating tumor DNA measurements as early outcome predictors in diffuse large B-cell lymphoma. J Clin Oncol. 2018 Oct 1;36(28):2845–53.
35. Roschewski M, Dunleavy K, Pittaluga S, Moorhead M, Pepin F, Kong K, et al. Circulating tumour DNA and CT monitoring in patients with untreated diffuse large B-cell lymphoma: A correlative biomarker study. Lancet Oncol. 2015;16(5):541–9.
36. Spina V, Bruscaggin A, Cuccaro A, Martini M, Trani M Di, Forestieri G, et al. Circulating tumor DNA reveals genetics, clonal evolution, and residual disease in classical Hodgkin lymphoma. Blood. 2018 May 31;131(22):2413–25.
37. Cheson BD, Fisher RI, Barrington SF, Cavalli F, Schwartz LH, Zucca E, et al. Recommendations for initial evaluation, staging, and response assessment of Hodgkin and non-Hodgkin lymphoma: the Lugano classification. J Clin Oncol. 2014 Sep 20;32(27):3059–67.
38. Dupuis J, Berriolo-Riedinger A, Julian A, Brice P, Tychyj-Pinel C, Tilly H, et al. Impact of [(18)F]fluorodeoxyglucose positron emission tomography response evaluation in patients with high-tumor burden follicular lymphoma treated with immunochemotherapy: a prospective study from the Groupe d'Etudes des Lymphomes de l'Adulte and GOELAMS. J Clin Oncol. 2012 Dec 10;30(35):4317–22.
39. Ansell SM, Armitage JO. Positron emission tomographic scans in lymphoma: convention and controversy. Mayo Clin Proc. 2012;87(6):571–80.
40. Galimberti S, Luminari S, Ciabatti E, Grassi S, Guerrini F, Dondi A, et al. Minimal residual disease after conventional treatment significantly impacts on progression-free survival of patients with follicular lymphoma: The FIL FOLL05 trial. Clin Cancer Res. 2014 Dec 15;20(24):6398–405.

41. Zohren F, Bruns I, Pechtel S, Schroeder T, Fenk R, Czibere A, et al. Prognostic value of circulating Bcl-2/IgH levels in patients with follicular lymphoma receiving first-line immunochemotherapy. Blood. 2015 Sep 17;126(12):1407–14.
42. Pott C, Hoster E, Kehden B, Unterhalt M, Herold M, van der Jagt RH, et al. Minimal Residual Disease in Patients with Follicular Lymphoma Treated with Obinutuzumab or Rituximab As First-Line Induction Immunochemotherapy and Maintenance in the Phase 3 GALLIUM Study. Blood. 2016 Dec 2;128(22):613–613.
43. Siva S, MacManus MP, Martin RF, Martin OA. Abscopal effects of radiation therapy: a clinical review for the radiobiologist. Cancer Lett. 2015 Jan 1;356(1):82–90.
44. Roschewski M, Rossi D, Kurtz DM, Alizadeh AA, Wilson WH. Circulating Tumor DNA in Lymphoma: Principles and Future Directions. Blood cancer Discov. 2022 Jan;3(1):5–15.
45. Scherer F, Kurtz DM, Newman AM, Stehr H, Craig AFM, Esfahani MS, et al. Distinct biological subtypes and patterns of genome evolution in lymphoma revealed by circulating tumor DNA. Sci Transl Med. 2016 Nov 9;8(364).

Tables

Table 1 is available in the Supplementary Files section.

Figures

Figure 1

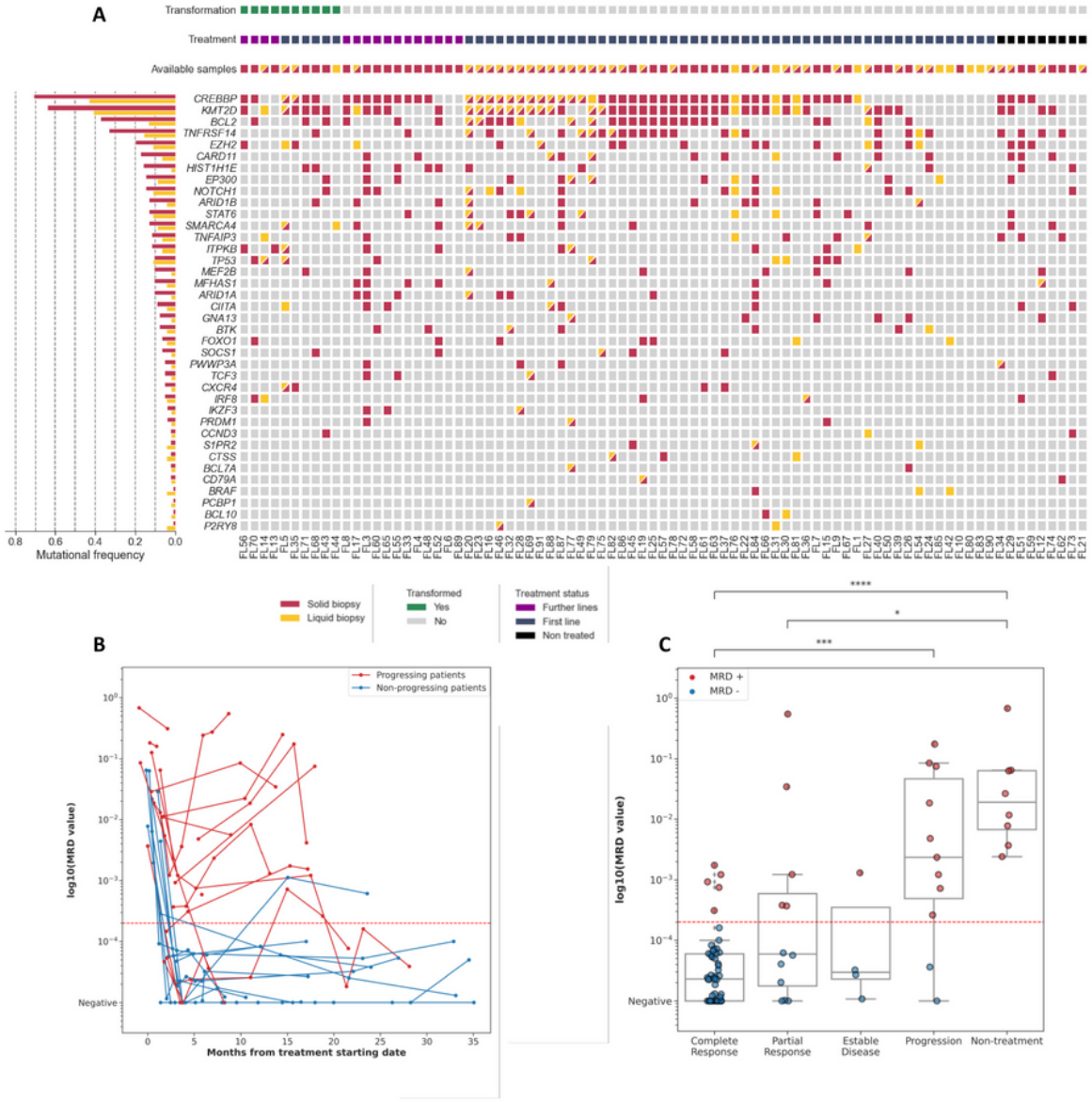

Figure 1

Baseline genotyping and potential of Liqbio-MRD to monitor disease progression: (**A**) Oncoplot of the baseline genotyping of 75 lymph node solid biopsy samples (red) and 44 plasma liquid biopsy samples (yellow). Patients are represented in the X-axis, genes in the Y-axis; (**B**) dynamics of cfDNA LiqBio-MRD in 55 FL patients, the LiqBio-MRD values for each follow-up datapoint (Y-axis) are plotted against the month

from treatment start (X-axis), patients that progressed are represented in red, complete and partial responses are represented in blue; (**C**) correlation of Liqbio-MRD and PET/CT.

Figure 2

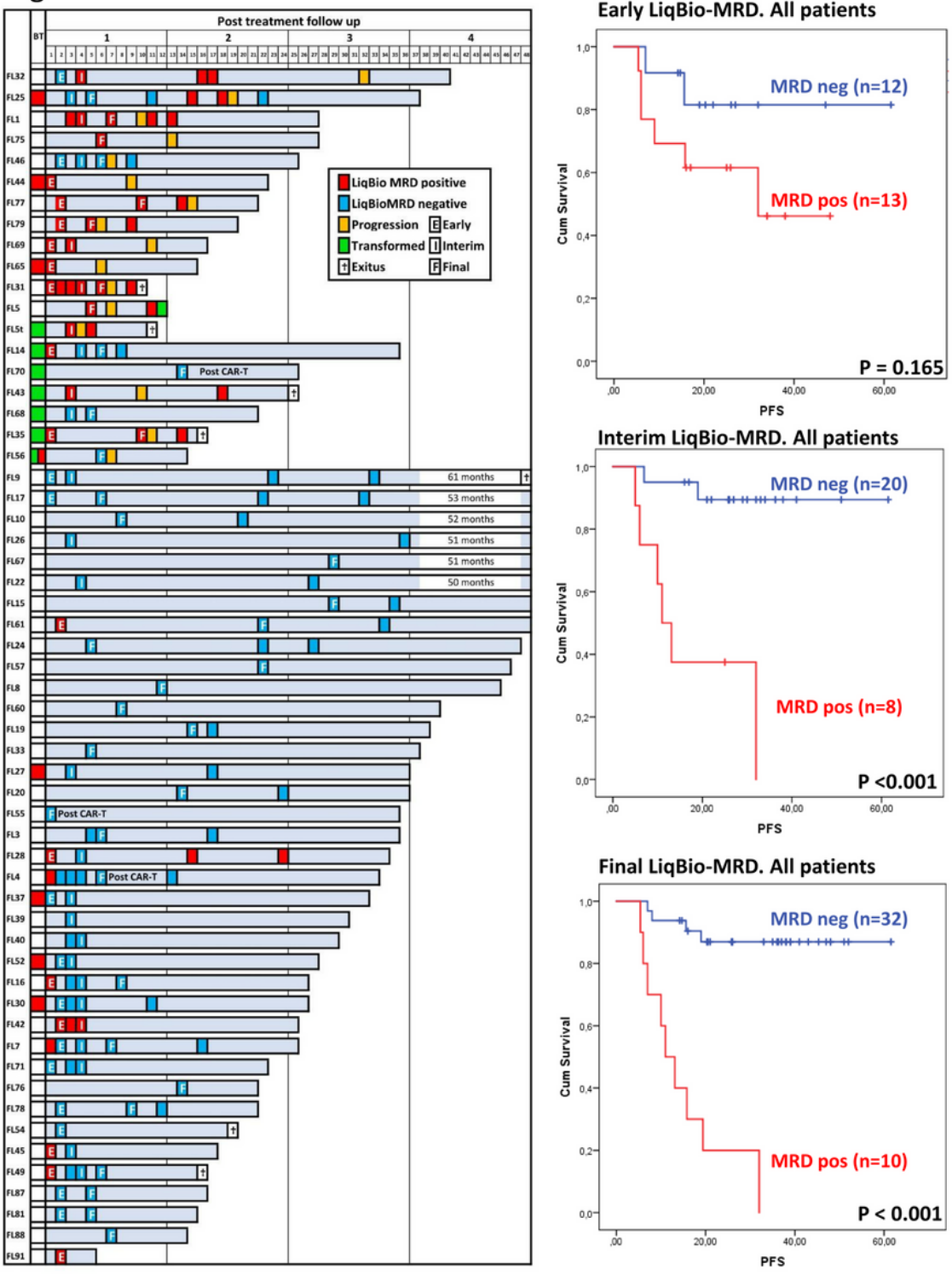

Figure 2

Clinical impact of early monitoring by LiqBio-MRD: (**left**) Swimmer plot of the different follow-up time-points screened for each patient. Red boxes represent time-points with positive MRD value. Blue boxes,

samples with negative MRD value. The samples used in the survival analysis at Early (E), Interim (I) and Final (or EOT, F) time-points are indicated for each patient. (**Right**) Kapplan–Mayer curves of the impact of LiqBio-MRD monitoring at the different time-points. These analyses were performed with all the patients under treatment, including transformed and relapsed patients.

Figure 3

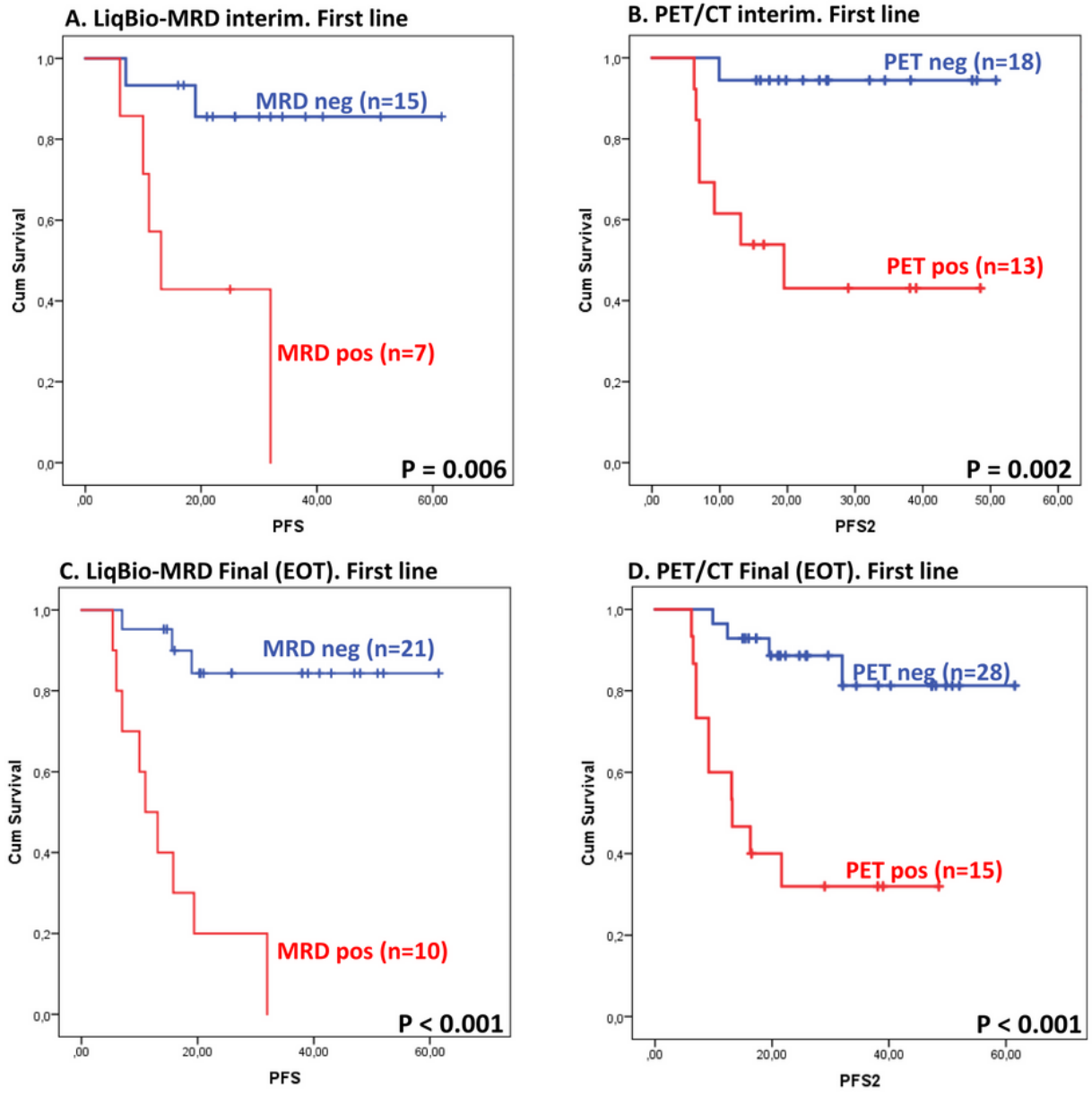

Figure 3

Interim monitoring by LiqBio-MRD and PET/CT predicts progression in first-line treated patients. Kaplan–Meier curves showing the impact of interim(**A**,**B**) and EOT (**C**,**D**) monitoring by LiqBio-MRD test **(A,C)** or PET/CT scan (**B,D**) in patients under first-line therapy. The same analyses excluding transformed cases are shown in Supplemental Figure S5.

Figure 4

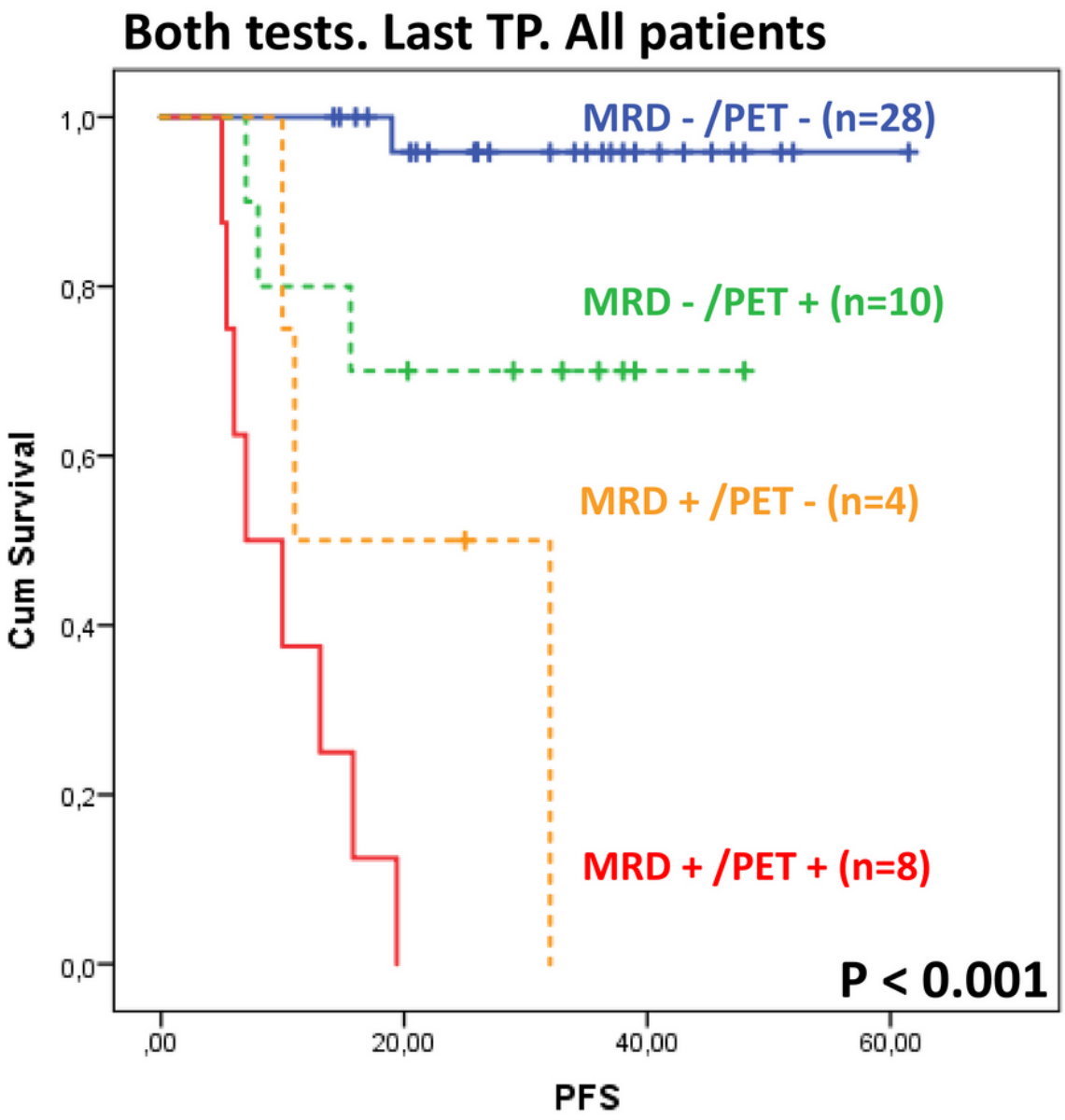

Figure 4

Clinical Impact of the LiqBio-MRD and PET/CT combination. Kaplan–Meier curves show the capacity to identify POD24 patients when both tests are combined. An analysis was performed using the last time-point with both determinations available (interim or EOT). The result only considering EOT and without relapse and transformed cases are shown in Supplemental Figure S6.

Figure 5

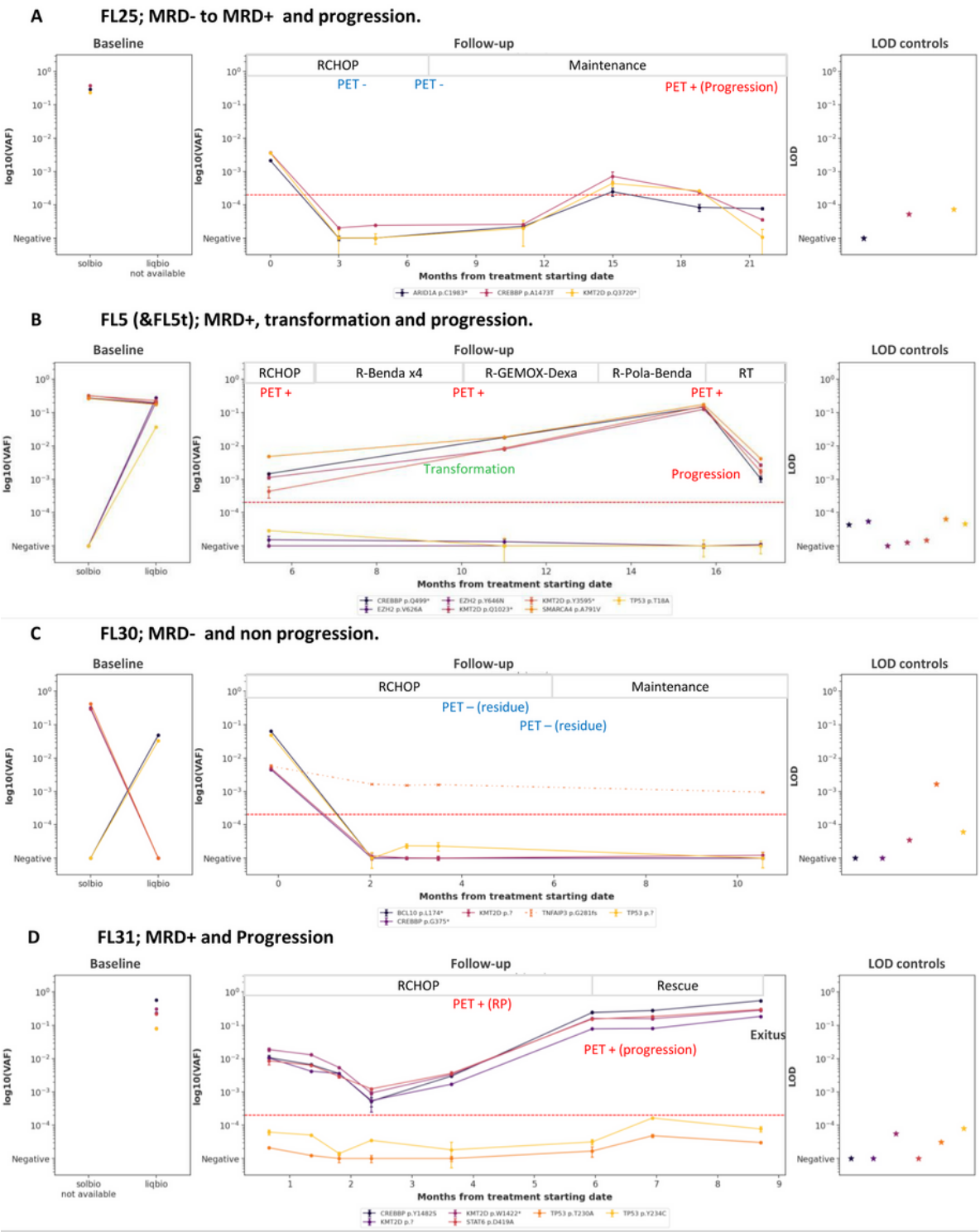

Figure 5

Examples of the Disease Dynamics monitored by LiqBio-MRD. The left panel represents the baseline genotyping of lymph nodes (SolBio) and/or plasma cfDNA (LiqBio) abtaining after applying the low sensitive targeted panel (sensitivity $2{\cdot}10^{-2}$). The panel in the middle represents the VAF values of the different mutations obtained by the ultrasensitive LiqBio-MRD test (sensitivity $2{\cdot}10^{-4}$). The right panel represents the limit of detection (LOD; mean + three standard deviations) defined in healthy control datapoints for every tracked mutation. Mutations with LOD above $1{\cdot}10^{-4}$, represented with dotted lines, were not used for MRD value calculation.

Supplementary Files

This is a list of supplementary files associated with this preprint. Click to download.

- Table1.xlsx
- Supplementalfigures.docx
- SupplementaltableS1.xlsx
- SupplementaltableS2.xlsx
- SupplementaltableS3.xlsx
- SupplementaltableS4.xlsx